

# Investigation of Microstrip Filters for Glucose and Tension Sensing Based on Biomedical Electronics

Shahad Khalid Khaleel

College of Engineering, University of Information Technology and Communications, Baghdad, Iraq

\*Corresponding author: [shahad.khalid@uoitc.edu.iq](mailto:shahad.khalid@uoitc.edu.iq)

Received Feb. 3, 2026

Revised Mar. 29, 2026

Accepted Jun.20, 2026

Online Jun. 24, 2026

## Abstract

The advantage of the microstrip filter-based sensing system is that it is planar, inexpensive, lightweight, and highly sensitive to electromagnetic fields, making it suitable for use in biomedical electronics. In this paper, microstrip technology is studied and applied to the design of glucose-sensing and tension-sensing filters, focusing on the sensing mechanisms, resonator geometries, operating frequency bands, type of substrate, fabrication procedure, and performance indicators. A comparative discussion is provided to illustrate the effects of field confinement, effective permittivity, and structural deformation on the resonance behavior. Recent developments of biosensors, flexible electronics, wearable electronics, and optimization techniques are also included. To make the paper more reproducible, a more complete nomenclature, the key equations used for the analysis, explicit simulation settings and additional result tables are added. Finally, some practical limitations, including calibration drift, environmental variation, hysteresis, and long-term stability are emphasized, and future trends in artificial intelligence, integration with the Internet of Things (IoT), metamaterial-inspired resonators, and flexible platforms using graphene are addressed.

**Keywords:** Biomedical electronics, microstrip filters, microwave sensors, glucose sensing, tension sensing, RF biosensors, wearable electronics, flexible sensors, resonators, microwave resonator sensors.

© The Author 2026.  
Published by ARDA.

## 1. Introduction

Compact planar structure and easy integration with peripheral components make microwave microstrip filters to be an important class of microwave components widely used in biomedical electronics, communication systems, radar technology, wireless devices and RF front-end systems [1, 2]. Such filters are now widely employed as physical and chemical sensors due to their resonant response which is very sensitive to environmental perturbations. Measurable resonance variations as a result of the change of dielectric properties, conductivity, or structural deformation can be regarded as strong sensing mechanisms. Glucose is considered one of the most critical biomedical applications of microwave sensing, and it is currently under study for non-invasive monitoring. Non-invasive glucose monitoring is currently being studied as one of the most critical biomedical applications of microwave sensing. Diabetes is one of the most common chronic conditions in the world, and it is important for people to monitor their blood or interstitial glucose levels continuously in order to manage their diabetes effectively. Traditional finger prick testing is invasive, can be uncomfortable and typically



decreases patient adherence. Planar microwave sensors are an interesting alternative, which track changes in the dielectric properties of biological tissues and fluids without chemical reagents, [3-6]. At the same time, there is tension sensing as another primary domain. The flexible microstrip filters are able to detect mechanical strains and physical deformations through changes in resonant frequency when their physical dimensions change. These sensors can thus be applied to smart clothing, robotics, structural health monitoring, biomedical rehabilitation platforms and wearable electronics [8-11].

Though this is the advantage, there are still some challenges like the need for a balance between sensitivity and robustness when deploying it in practice. Glucose sensors need to be highly responsive to the glucose solution and, at the same time, be stable to temperature, hydration and motion artifacts. Tension sensors have to exhibit measurable frequency changes when strained and repeatable during repeated loadings. All these conflicting requirements drive a careful selection of resonators, engineering of the substrate, and signal processing support. Again, the microstrip filters are particularly appealing for this application because they can be fabricated with conventional board fabrication techniques and integrated into both rigid and flexible platforms at low-cost.

## 2. Fundamental Theory of Microstrip Filter Sensors Based on Biomedical Electronics

A microstrip filter is a conducting metallic structure that is patterned on a dielectric material over a ground plane. Resonant properties are functions of resonator size, the dielectric constant of the substrate, the geometry of the conductors and the coupling conditions. The electromagnetic field distribution of microstrip resonators is very sensitive to the characteristics of materials around the resonator [12, 13, 14].

One of the popular sensing mechanisms is called the perturbation method. A shift in effective permittivity due to the presence of a surrounding dielectric material (or due to deformation of the resonator geometry) causes a resonant frequency shift. Resonant frequency, return loss, insertion loss, quality factor, and coupling coefficient are the most common parameters monitored. In practice, these quantities are combined and used together because the interaction between them, frequently, unlocks the sensing mechanism more clearly.

In recent development, microwave planar resonators are found to be very successful transducers in non-invasive and biomedical sensing. These features are used in glucose monitoring systems to take advantage of the high sensitivity of the electromagnetic response to the surroundings. The device changes the complex permittivity of the medium when a biological sample or a glucose solution is added in the localized sensing region, resulting in a variation of its capacitance or electrical length. This physical change is manifested as a detectable change in resonant frequency, amplitude or phase. Furthermore, the loaded quality factor can also show the sensitivity of the resonator to small changes, which is beneficial if the concentration of the resonator is to be varied within a small range.

Split Ring Resonator (SRR) is a device comprising of concentric metallic rings with carefully designed gaps on a dielectric material. The narrow gaps generate a high capacitive effect, and the uninterrupted metallic path of the inner and outer rings offer an inductive effect. This LC behavior gives rise to a very strong electric field in the gap region, rendering the SRR sensitive to the changes in the surrounding dielectric medium. Consequently, the permittivity changes in the sample, in the case of glucose, can cause a good response in the SRR-based sensor when the sample is placed directly above the split region.

The Complementary Split Ring Resonator (CSRR) is a dual version of SRR which is directly etched into the ground plane instead of printing the metallic rings on the substrate. In the case of the CSRR, the mechanism of excitation is different from the SRR, it is mainly excited by an electric field normal to the plane. The etched slots create a high electric field concentration in a very small region, thereby resulting in a highly sensitive sensor for biomedical sensing of liquids, chemicals, and subsurface.

The straight half-wavelength microstrip resonator is folded into an elegant Hairpin Resonator. These folding decreases the footprint but keeps the same electrical length for resonance. Inter-arms coupling is strong, due to the nearness of the two parallel arms, affecting the distributed capacitance and inductance of the structure. This

peak is very sharp and stable and is shifted in predictable ways when a sample of glucose alters the effective permittivity of the vicinity.

Stub Resonator is a very simple open-ended (or short circuit) transmission-line section that is connected at right angles to the main feedline. The stub is usually a quarter wavelength or half wavelength long. It creates a standing-wave pattern with a known location of the field maximum, and a target analyte in the vicinity of the open end changes the local capacitive loading. This loading affects the electrical length of the stub and the resulting change in the measured reflection coefficient (S11) or transmission coefficient (S21) is suitable for concentration mapping.

An alternative approach for the sensor is to take advantage of a microstrip transmission line structure connected to an asymmetric defected ground structure of double nested complementary split-ring resonators [5,6]. The system is flexibly designed on an elastomer with thickness  $h$  and relative permittivity  $\epsilon_r$ . When there is no strain, the effective dielectric constant  $\epsilon_{eff}$  and the characteristic impedance  $Z_0$  can be estimated by conformal mapping and the quasi-static approximation [2].

$$\epsilon_{eff} = \frac{\epsilon_r + 1}{2} + \left(\frac{\epsilon_r - 1}{2}\right) * \left[1 + 12 * \left(\frac{h}{W}\right)\right]^{-0.5} + F(\epsilon_{strain})$$

$$Z_0 = \frac{120\pi}{\left\{\sqrt{\epsilon_{eff}} * \left[\frac{W}{h} + 1.393 + 0.667 * \ln\left(\frac{W}{h} + 1.444\right)\right]\right\}}$$

An aqueous glucose solution results in a dispersive Debye relaxation profile in the complex permittivity as it loads the sensor. This change alters the fundamental resonance frequency  $f_{r1}$ , which creates a direct tracking pathway for biological systems [1]. The primary design goal is to maximize the overlap between the sensing field and the material being tested with unwanted fringing as minimally as possible out of the measurement region.

$$f_{r1}(C_{glu}) = \frac{1}{\left[2\pi * \sqrt{L_{eq} * (C_{sub} + \eta * \Re\{\epsilon * (\omega, C_{glu})\}) * C_{fringe}}\right]}$$

At the same time, the geometry of the sensor on the longitudinal axis changes due to the mechanical strain. Under loading, the physical size changes, depending on the substrate Poisson's ratio  $\nu$ . These geometric changes alter the secondary resonant loop's distributed inductance  $L_{strain}$  and capacitance  $C_{strain}$  which then shifts the secondary resonant mode  $f_{r2}$  independent of the primary biological mode [7]. The value of the separation of two resonant modes is that it provides more reliable separation of the strain and glucose effects.

$$f_{r2}(\epsilon_x) = \frac{1}{\left[2\pi * \sqrt{L_{strain}(\epsilon_x) * C_{strain}(\epsilon_x)}\right]}$$

The working principle of planar microwave sensors for biochemical monitoring (e.g., glucose monitoring) is based on the theory of electromagnetic perturbation [22,23]. By placing a dielectric material under test over a microstrip resonator, the fringing electric field affects the properties of the material [23]. This change alters the basic resonant frequency of the system. Bethe-Schwinger perturbation theory states that the shift in resonant frequency of a dielectric perturbation is proportional to the ratio of the stored electric energy in the resonant volume to the total energy of the field in the volume [24]. That is why, in the case of a resonator designed to have strong field confinement, small samples can give measurable responses.

$$\frac{\Delta f}{f_0} = - \left( \int_V \Delta \epsilon * E_0 \cdot E_1 dA \right) / \left( \int_V (\epsilon_0 * |E_0|^2 + \mu_0 * |H_0|^2) dA \right)$$

where  $E_0$  is the unperturbed electric field vector and  $H_0$  is the unperturbed magnetic field vector and  $E_1$  is the perturbed electric field vector after the material is inserted [24]. In planar microstrips with thin microstrip structure where the material target is placed on top of the microstrip, the system can be modeled by introducing an effective dielectric constant  $\epsilon_{eff}$  [25]. The half-wavelength microstrip line has the fundamental resonant frequency  $f_0$  of:

$$f_0 = \frac{c}{(2 * L * \sqrt{\epsilon_{eff}})}$$

The blood or interstitial fluid glucose concentration will affect the permittivity of the tissue layer [22] due to the complex nature of the permittivity. This modification alters the effective dielectric constant of the microstrip system, and thus the resonant frequency. If the variation of the dielectric is small compared to the background permittivity, then the shift can be approximated with a first order Taylor expansion for the case of a half-wavelength resonator [25]. This is typically negative, so that a higher permittivity corresponds to a lower resonance frequency.

$$f_0 + \Delta f = \frac{c}{(2 * L * \sqrt{\epsilon_{eff} + \Delta\epsilon_{eff}})} = f_0 * \left(1 + \frac{\Delta\epsilon_{eff}}{\epsilon_{eff}}\right)^{-\frac{1}{2}} \approx f_0 * \left(1 - \frac{\Delta\epsilon_{eff}}{(2 * \epsilon_{eff})}\right)$$

When the frequency shift is isolated, it becomes clear that it follows a mathematical relationship that allows us to understand why the transmission resonance decreases with the increase of the dielectric constant or the amount of glucose [24]:

$$\Delta f = -f_0 * \frac{\Delta\epsilon_{eff}}{(2 * \epsilon_{eff})}$$

The main analytical relations used throughout the paper are summarized below for clarity:

$$\text{Equation (1): } f_0 = \frac{c}{(2L\sqrt{\epsilon_{eff}})}$$

$$\text{Equation (2): } f_r = \frac{1}{(2\pi\sqrt{LC})}$$

$$\text{Equation (3): } \Delta f / f_0 \approx -0.5 \cdot (\Delta\epsilon / \epsilon_{eff})$$

$$\text{Equation (4): } \epsilon_{eff} \approx \frac{\epsilon_r + 1}{2} + \frac{\epsilon_r - 1}{2} \cdot \frac{1}{\sqrt{1 + \frac{12h}{w}}}$$

$$\text{Equation (5): } L_{strain} = L_0(1 + \epsilon_s), W_{strain} = W_0(1 - \nu\epsilon_s)$$

Alternatively, the field interactions of planar resonators can be converted to familiar electrical components (inductance and capacitance) in a lumped-element equivalent circuit model. An SRR is mainly based upon magnetic coupling and can be modeled as an LC tank circuit in parallel with the transmission line with a mutual inductance. On the other hand, a CSRR is an electric-field coupled device, and typically consists of a series LC tank circuit coupled by a capacitance  $C_c$ .

$$f_0 = \frac{1}{(2 * \pi * \sqrt{L_{eq} * C_{eq}})}$$

When a biochemical target is placed over a CSRR, the material will change the equivalent capacitance of the sub-wavelength slot. This variation changes the resonant frequency due to the field being confined to a very small physical volume [24]. This gives a robust and measurable response even to minor variations in the surrounding dielectric environment.

$$f_{0,perturbed} = \frac{1}{(2 * \pi * \sqrt{L_{eq} * (C_0 + C_{material})})}$$

The lump formulation is able to account for this and is the reason the CSRR configuration is very sensitive to the dielectric changes. Because of its slot geometry it is very well suited to concentrating the electric field lines into a small area and hence any small change in the material results in a measurable change in the overall equivalent capacitance [25]. In terms of design, this is one of the major advantages of CSRR structures for high sensitivity liquid sensing.

These microstrip structures can be automatically designed by combining the mathematical models with full-wave electromagnetic solvers using a Hybrid Genetic Particle Swarm Optimization (HGPSO) algorithm [1-15]. The optimization engine is able to manipulate geometric parameters like the width of the slot, the position of the feed and the length of the patch, to meet a set of desired performance metrics over a specified operating band. This optimization is especially useful when multiple objectives must be optimized simultaneously, like sensitivity, footprint and fabrication tolerance.

---



---

#### Algorithm 1: Hybrid Genetic Particle Swarm Optimization for Microstrip Sensors

---



---

Input : Swarm Size (N), Max Generations ( $t_{max}$ ), Parameter Bounds [ $X_{min}$ ,  $X_{max}$ ]

Output: Optimized Geometric Parameter Vector ( $g_{best}$ )

---

```

1: Initialize population positions  $x_i$  and velocities  $v_i$  randomly within bounds
2: Map initial parameter vectors  $x_i$  to EM solver geometric models
3: Execute full-wave EM simulations for the initial population
4: Calculate initial fitness  $F(x_i)$  using the multi-objective fitness equation
5: Set  $p_{best,i} = x_i$  and assign  $g_{best} = \text{argmin}(F(x_i))$ 
6: Set  $stagnation\_counter = 0$ 
7: for  $t = 1$  to  $t_{max}$  do
8:   Calculate non-linear dynamic inertia weight  $w(t)$  via sine adjustment
9:   for each particle  $i$  from 1 to N do
10:    Update velocity vector  $v_i(t+1)$  using cognitive and social constraints
11:    Enforce velocity boundary clipping: if  $v_i > v_{max}$  then  $v_i = v_{max}$ 
12:    Update position vector  $x_i(t+1) = x_i(t) + v_i(t+1)$ 
13:    Enforce position boundary constraints within [ $X_{min}$ ,  $X_{max}$ ]
14:   end for
16:   Execute automated EM solver batch pipeline for new particle configurations
17:   Extract extracted S11, VSWR, and efficiency profiles from EM outputs
18:
19:   for each particle  $i$  from 1 to N do
20:    Evaluate multi-objective fitness  $F(x_i(t+1))$ 
21:    if  $F(x_i(t+1)) < F(p_{best,i})$  then
22:       $p_{best,i} = x_i(t+1)$ 
23:    end if
24:   end for
25:
26:   Identify current population minimum candidate:  $current\_best$ 
27:   if  $F(current\_best) < F(g_{best}) - \Delta_{psi}$  then
28:      $g_{best} = current\_best$ 
29:      $stagnation\_counter = 0$ 
30:   else
31:      $stagnation\_counter = stagnation\_counter + 1$ 
32:   end if
33:
34:   if  $stagnation\_counter \geq 5$  then
35:     Sort swarm particles based on fitness scores
36:     Retain top 70% of elite particles unmodified
37:     Apply Tournament Selection to replace bottom 30% of stagnant population
38:     Perform arithmetic crossover on selected parents to yield new offspring

```

---

```

39:   Apply uniform mutation operator to offspring parameters
40:   Re-initialize velocity fields for mutated offspring particles
41:   stagnation_counter = 0
42:   end if
43: end for
44: return g_best
    
```

Table 1 compares their principal sensing trade-offs, while Figure 1 summarizes the SRR, CSRR, hairpin, and stub resonators.

Table 1. Comparison of Glucose Sensing Resonator Structures

Structure	Employed Frequency	Sensitivity	Advantages	Limitations
SRR	2.4 GHz	High	Compact and sensitive	Affected by environmental noise
CSRR	5.8 GHz	Very High	Strong field confinement	Complex fabrication
Hairpin	3.5 GHz	Moderate	Miniaturized design	Lower Q-factor
Stub-loaded	24 GHz	Excellent	Millimeter-wave precision	High cost

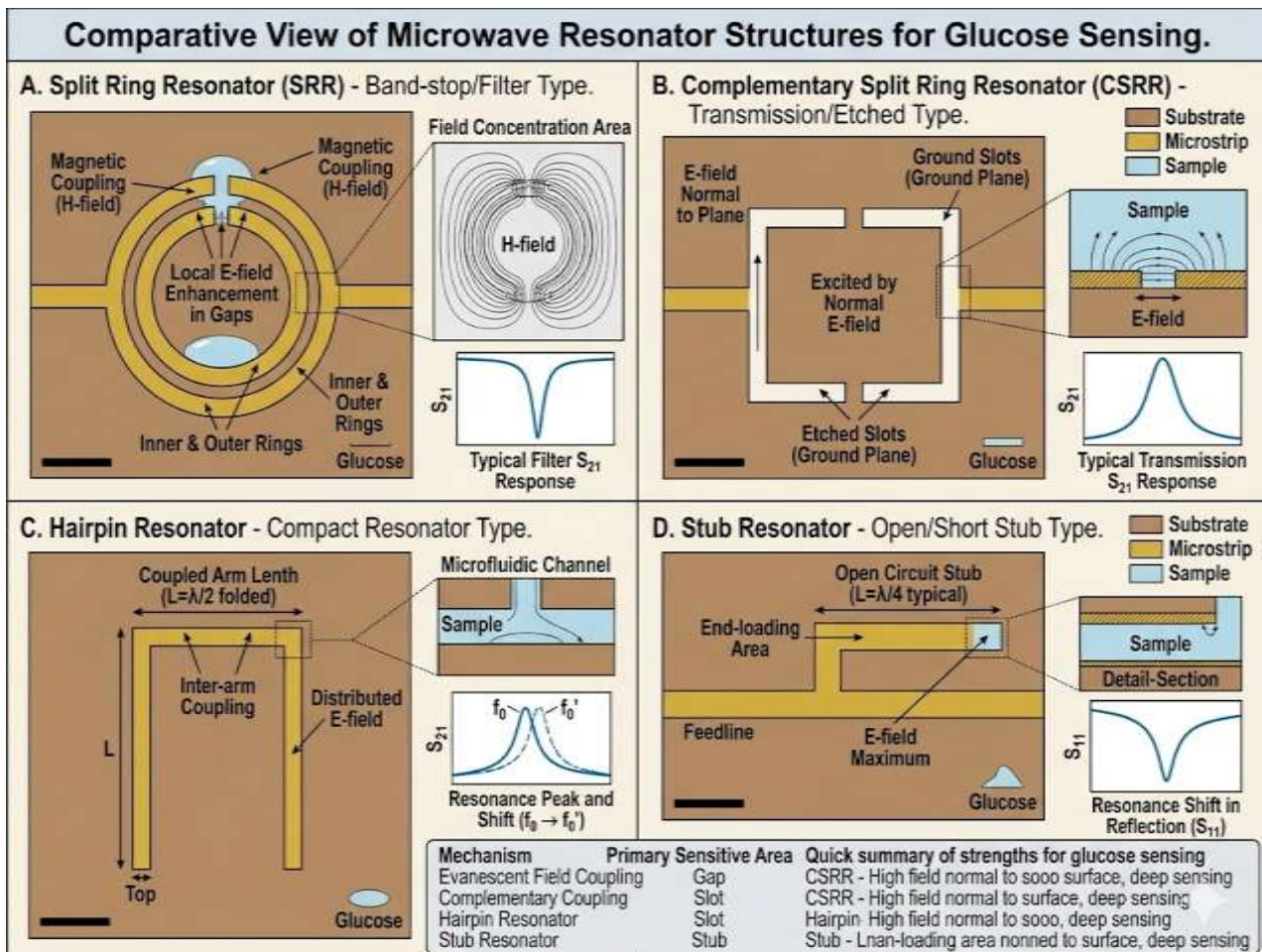


Figure 1. Summary about the investigated Split Ring Resonator (SRR), the Complementary Split Ring Resonator (CSRR), the Hairpin Resonator, and the Stub Resonator.

### 3. Results and discussion

The concept of the Glucose sensing system by Microwave is to measure the changes in the dielectric properties of biological sample. Glucose concentration affects the dielectric constant and blood or interstitial fluid (ISF) conductivity, which affects the resonator's electromagnetic response [4-9]. Thus, the response summarized in Fig. 2 will be related to the effective permittivity change, and the comparative interpretation outlined in Table 1 will be retained since the optimal resonator type will depend on the bandwidth, field confinement, fabrication tolerance and range of expected measurement.

In the literature, several resonator structures have been proposed including split-ring resonator (SRR), complementary split-ring resonator (CSRR), interdigital resonator, hairpin filter, stub loaded structure, and open-loop resonator. The SRR and CSRR geometries in particular are very appealing due to their high sensitivity and good field confinement. Operating at higher frequencies is generally more sensitive due to increased electromagnetic interaction with biological materials, but there also are increases in the material attenuation and increased complexity in the fabrication. Hence, the study of compact resonators with a desired sensitivity in the low to mid-GHz band has been the subject of many recent investigations [1, 2, 12-15] and then introduced to millimeter-wave operation.

As well as frequency choice calibration is key. The temperature, hydration and composition of biological samples all affect the effect they have on biological samples, so a glucose sensor should not be dependent on resonance shift without compensation. Therefore, in practical systems a baseline signal is combined with reference resonators and multivariate interpretation methods to separate glucose-induced changes from background variations. The settings in the representative plots are included in Table 6 for reproduction of the comparative results. The representative numbers shown in Table 2 are used for comparison. As is expected, Figure 2 displays an expected shifting resonance as a function of the increasing concentration of glucose. Under the conditions given in Table 2, glucose-sensing results are representative and shown in Table 3.

Table 2. Representative Simulation Settings Used to Generate the Comparative Results

Parameter	Setting	Purpose
EM solver	CST Microwave Studio	Full-wave verification
Frequency sweep	1–30 GHz	Cover low- and high-band resonances
Boundary condition	Open add space	Reduce boundary reflection
Excitation	Waveguide port	Standard S11/S21 extraction
Substrate	RO4003, $\epsilon_r = 3.55$	Reference glucose-sensor platform
Flexible substrate	PDMS / PET / textile	Reference tension-sensor platform
Glucose loading range	50–300 mg/dL	Representative dielectric variation
Strain range	0–30%	Representative mechanical loading

Table 3. Representative Glucose-Sensing Results Under the Settings in Table 2

Glucose (mg/dL)	Resonance Frequency (GHz)	Frequency Shift (MHz)	Relative Sensitivity (MHz/mg/dL)
50	2.40	0	0.0
100	2.30	-100	2.0
150	2.20	-200	2.0
200	2.10	-300	2.0
250	2.00	-400	2.0
300	1.90	-500	2.0

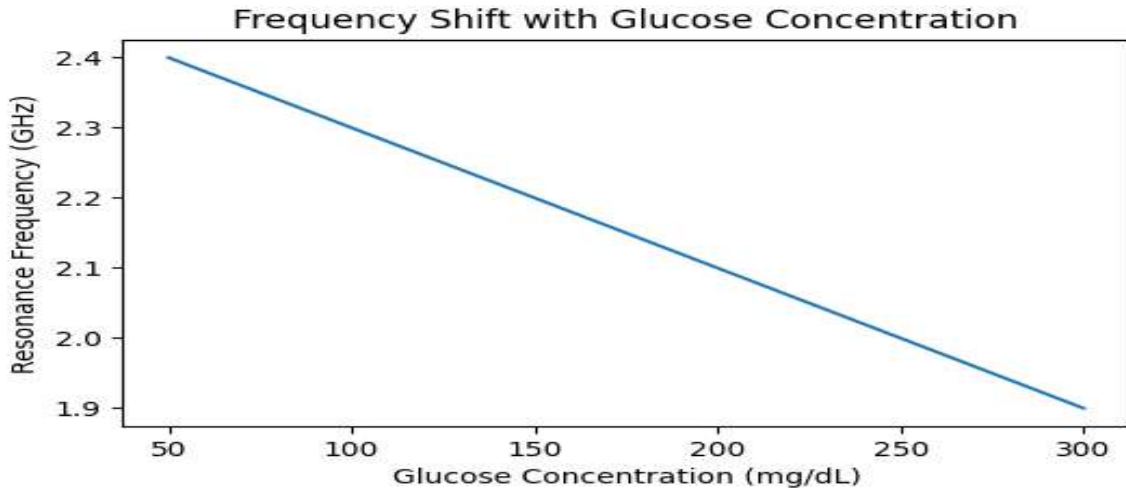


Figure 2. Resonance frequency shift caused by glucose concentration variation.

The flexible microwave tension sensors are made by deforming the geometry of the resonator under tension. The resonant frequency is a measurable parameter which changes as a result of the changes in resonator electrical length and current distribution induced by stretching [10-15]. The monotonic frequency reduction under strain summarized in figure 3, and the representative values for the stretched configuration are summarized in table 8.

As flexible substrates like PDMS, PET, polyimide and textile materials can bend and stretch without unacceptable degradation of RF performance, they are popular. These sensors have recently been incorporated into wearable systems for motion tracking, posture monitoring and healthcare applications. However, for wearable applications, other performance factors such as substrate comfort, breathability, and washability may be as critical as electromagnetic performance.

Preferably, the tension sensor should be highly sensitive, have low hysteresis, high repeatability and a long life. Studies are currently underway to develop greater mechanical stability and durability with repeated deformation cycles. In practice, a compromise of stretchability versus degree of post loading geometric recovery is often necessary.

The summary of the trends in Figure 3 is used for comparative analysis, and the settings and output are shown in Table 4. The comparison of the adopted flexible substrate of the tension sensors is shown in Table 5.

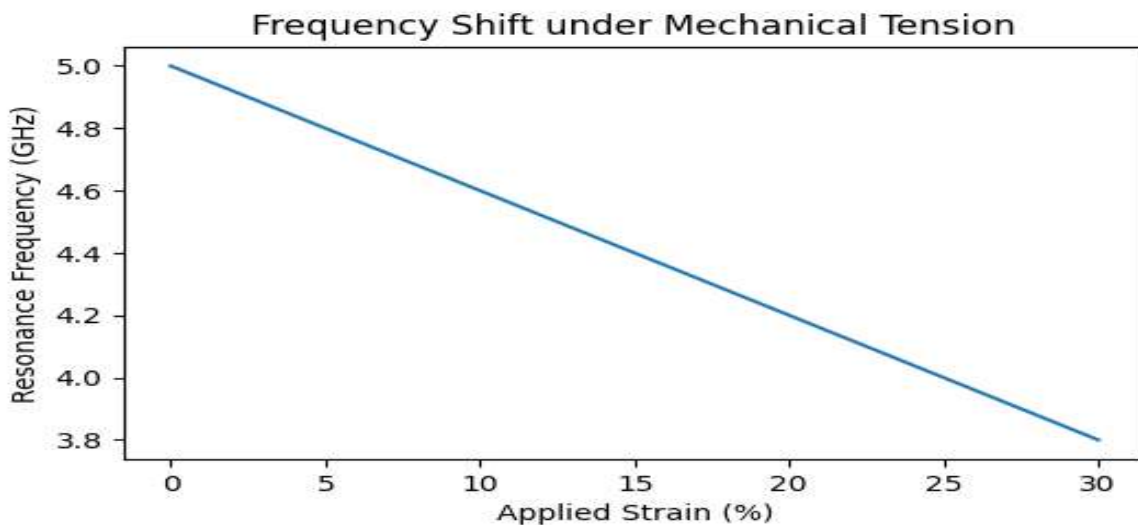


Figure 3. Simulated resonance frequency variation under mechanical tension.

Table 4. Representative Tension-Sensing Results Under the Settings in Figure 3

Applied Strain (%)	Resonance Frequency (GHz)	Frequency Shift (GHz)	Relative Sensitivity (GHz/%)
0	5.00	0.00	0.000
5	4.80	-0.20	0.040
10	4.60	-0.40	0.040
15	4.40	-0.60	0.040
20	4.20	-0.80	0.040
25	4.00	-1.00	0.040
30	3.80	-1.20	0.040

Table 5. Flexible Substrate Comparison for Tension Sensors

Substrate	Flexibility	Durability	Stretchability	Application
PDMS	Excellent	Moderate	Very High	Wearable devices
Polyimide	High	Excellent	Moderate	Flexible circuits
PET	Moderate	High	Low	Structural monitoring
Textile	Very High	Moderate	High	Smart clothing

Microstrip filter Sensor is a research method with a number of advantages, such as small size, low power consumption, wireless work and real-time sensing. The high-field resonator structures provide increased sensitivity for glucose sensing, flexible substrates for mechanical adaptability for tension sensing applications. Figures 2 and 3 show the anticipated frequency trends, while Figures 4 and 5 provide a summary of resonator performance.

The operating frequency, resonator geometry and substrate material are important parameters for the performance of a glucose sensor. Similarly, flex, mechanical strength, and resonance stability affect the performance of the tension sensor. The optimal resonator architecture and substrate are most often designed as a coupled system.

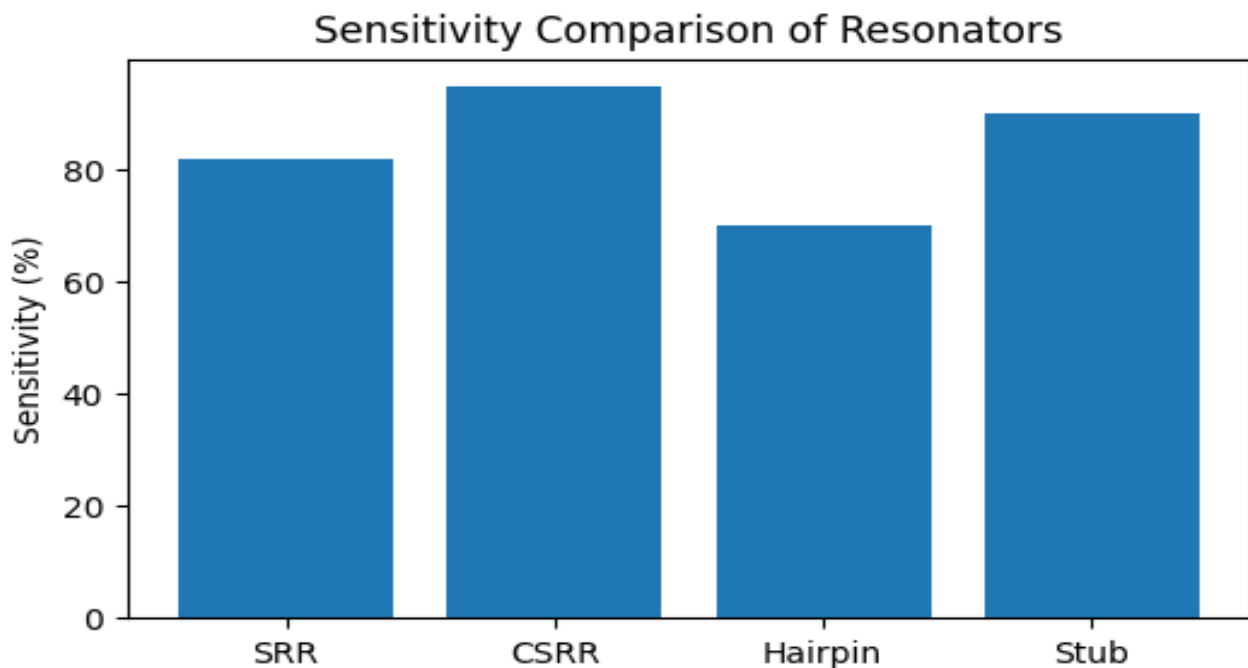


Figure 4. Sensitivity comparison of common resonator structures.

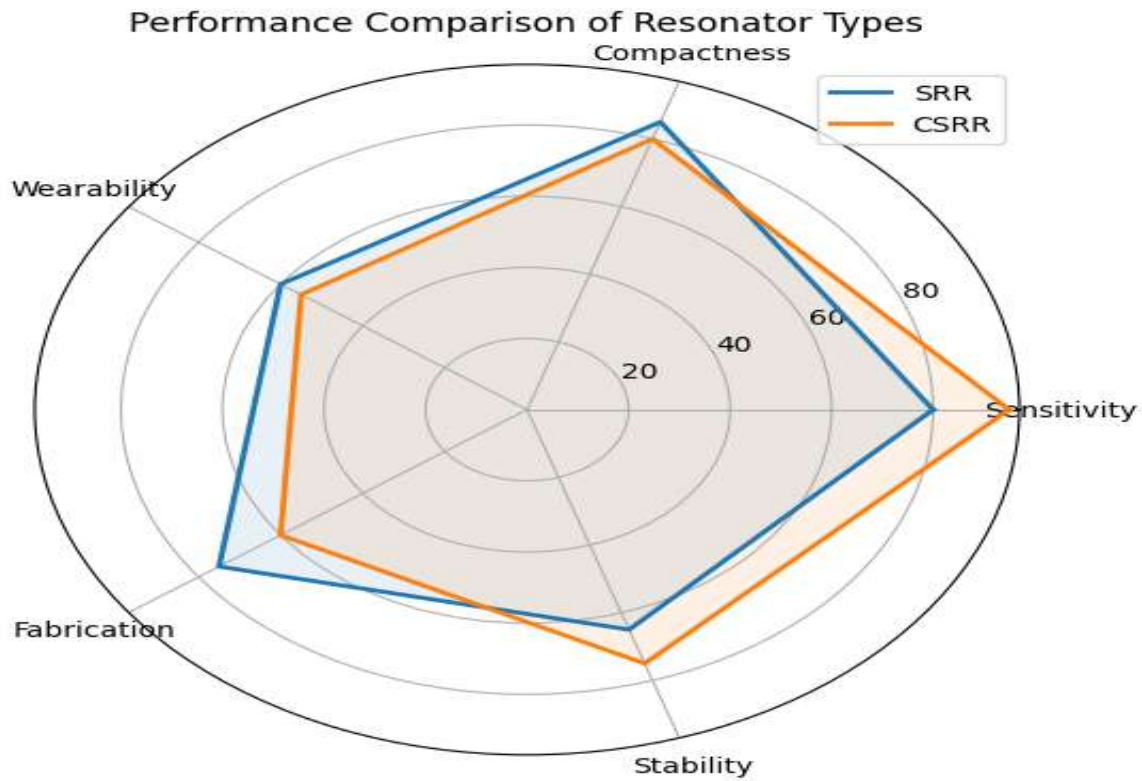


Figure 5. Radar depiction for comparing the performance of investigated resonators

The comparative results are summarized in Table 6 and Table 7, and the primary design gaps found in the literature are listed. Table 8 provides the extended outcomes for glucose and tension sensing, respectively.

Table 6. Advantages and Limitations of Microstrip Filter Sensors

Aspect	Advantages	Limitations
Compactness	Portable systems	Miniaturization complexity
Sensitivity	High detection accuracy	Environmental sensitivity
Fabrication	Low-cost PCB manufacturing	Precision required
Wearability	Flexible integration	Mechanical fatigue
Wireless Integration	Remote monitoring capability	Power management issues

Table 7. Key Research Gaps and Mitigation Strategies

Challenge	Effect on Measurement	Mitigation Strategy	Expected Benefit
Temperature variation	Baseline resonance drift	Reference resonator and calibration	Higher accuracy
Mechanical hysteresis	Reduced repeatability	Encapsulation and strain isolation	Stable output
Fabrication tolerance	Frequency offset	EM optimization and tolerance analysis	Improved yield
Sample variability	Signal fluctuation	Surface treatment and multivariate processing	Better robustness
Wireless power limits	Reduced operating range	Efficient readout and energy harvesting	Longer autonomy

Tables 8. The extended consequences for glucose and tension sensing, respectively.

Sensor Category	Preferred Structure or Substrate	Main Strength	Main Limitation	Typical Application
Glucose sensing	CSRR / SRR	Strong dielectric interaction	Temperature drift	Non-invasive monitoring
Tension sensing	PDMS-based flexible resonator	Large strain response	Hysteresis	Wearables and motion tracking
Hybrid multifunction sensing	Dual-mode DGS or multi-resonator	Simultaneous measurands	Decoupling complexity	Smart textiles
High-frequency sensing	Stub-loaded mm-wave	High resolution	Fabrication cost	Laboratory validation

There are a number of important developments in the field of microwave sensing technology based on microstrip filters as revealed in the literature. In the past, non-invasive glucose sensing systems have been demonstrated to have great potential for use with dielectric characterization techniques. However, biological tissues are complex and several factors in the environment may introduce error in the measurement, such as temperature, hydration-level, humidity, and movement. That's why the calibration and compensation strategy.

Furthermore, the flexible microwave tension sensors have demonstrated good performance in the area of wearable devices and robots. Multiple stretching cycles, however, can result in mechanical hysteresis, frequency drift and material fatigue. Thus, long-term reliability relies on the use of better flexible materials, better bonding techniques and better fabrication techniques.

The increased glucose concentration leads to a decreased resonance frequency due to the increase in the dielectric permittivity surrounding the resonator, resulting in change of its effective electrical length and electromagnetic propagation characteristics. The enhanced electric field confinement and stronger interaction between the electric field and the sensing medium is the reason for the higher sensitivity of the CSRR structure. When mechanical deformation occurs, the frequency drift in flexible resonators is also measurable, due to the change in the current path and the resonant dimensions. These trends reinforce those noted in Figures 2, 3, 4 and 5.

#### 4. Conclusion and future scope

Microstrip filter technology is a promising option for glucose sensing and tension sensing applications, due to its small geometry, high sensitivity, low cost and flexibility with flexible electronics. In the biomedical monitoring and wearable systems, resonator-based microwave sensors have great potential, particularly for non-invasive measurements. Improvements in sensing capability are expected in the future, with progress in meta-materials, flexible electronics and artificial intelligence being important factors.

The use of AI algorithms with microwave sensing technologies will be expected to increase in the future for greater accuracy, reliability and automation. AI-driven signal processing techniques can aid in calibration, account for temperature and humidity changes, and aid in data interpretation. In addition, IoT communication technologies will be integrated with sensing platforms, allowing for remote diagnostics and intelligent monitoring systems. Other future directions include the development of flexible and biodegradable substrates for use in biomedical applications, miniaturized resonators based on graphene for operation at millimeter-wave and terahertz frequencies for increased resolution, and energy harvesting approaches to achieve autonomous operation, in addition to the development of platforms that can collect multiple parameters, such as glucose, temperature, strain and other physiological or mechanical variables.

## Declaration of competing interest

The authors declare that they have no known financial or non-financial competing interests in any material discussed in this paper.

## Funding information

No funding was received from any financial organization to conduct this research.

## References

- [1] D. M. Pozar, *Microwave Engineering*, 4th ed. Hoboken, NJ, USA: Wiley, 2011.
- [2] J. S. Hong and M. J. Lancaster, *Microstrip Filters for RF/Microwave Applications*. New York, NY, USA: Wiley, 2001.
- [3] Martins, A. J., Velasquez, R. J., Gaillac, D. B., Santos, V. N., Tami, D. C., Souza, R. N., ... & Ramirez, J. C. (2025). A comprehensive review of non-invasive optical and microwave biosensors for glucose monitoring. *Biosensors and Bioelectronics*, 271, 117081.
- [4] EZarifi, M. H., Thundat, T., & Daneshmand, M. (2015). High resolution microwave microstrip resonator for sensing applications. *Sensors and Actuators A: Physical*, 233, 224-230.
- [5] Tahmid, A., Rahman, T., Emam, S. A., Reza, S. M., Hosen, M. I., Inum, R., & Habib, A. (2024). Low-cost and easy-to-fabricate microwave sensor for sensitive glucose monitoring: A step towards continuous glucose monitoring. *IEEE Journal of Electromagnetics, RF and Microwaves in Medicine and Biology*, 9(2), 221-228.
- [6] Costanzo, S. (2017). Non-invasive microwave sensors for biomedical applications: New design perspectives. *Radioengineering*, 26(2), 406-410.
- [7] Jang, C., Lee, H. J., & Yook, J. G. (2021). Radio-frequency biosensors for real-time and continuous glucose detection. *Sensors*, 21(5), 1843.
- [8] Reyes-Vera, E., Montoya-Villada, S., Umaña-Idarraga, F., Bedoya-Londoño, S., Araujo-Muñoz, J., & Ossa-Molina, O. (2024). High-sensitivity strain sensing using a flexible microstrip antenna with metamaterial resonator. *IEEE Sensors Journal*, 25(1), 647-654.
- [9] Luo, Q., Ji, W., Yin, Y., Chen, Z., Zhu, J., Li, L., & Chen, G. (2025). Enabling flexible, wearable, and implantable electronics with radio frequency-based wireless charging: Fundamentals, challenges, and emerging applications. *FlexMat*, 2(4), 493-509.
- [10] Alsultani, A. B., Kovács, K., Chase, J. G., & Benyo, B. (2025). Advances in invasive and non-invasive glucose monitoring: A review of microwave-based sensors. *Sensors and Actuators Reports*, 9, 100332.
- [11] Costanzo, Alessandra, et al. "Microwave devices for wearable sensors and IoT." *Sensors* 23.9 (2023): 4356.
- [12] Wang, Yun Xiu, et al. "Dual-band bandpass filter design using stub-loaded hairpin resonator and meandering uniform impedance resonator." *Progress In Electromagnetics Research Letters* 95 (2021): 147-153.
- [13] Martín, F., & Bonache, J. (2014). Application of RF-MEMS-based split ring resonators (SRRs) to the implementation of reconfigurable stopband filters: a review. *Sensors*, 14(12), 22848-22863.
- [14] K. C. Gupta et al., *Microstrip Lines and Slotlines*. Norwood, MA, USA: Artech House, 1996.
- [15] Caloz, Christophe, and Tatsuo Itoh. *Electromagnetic metamaterials: transmission line theory and microwave applications*. John Wiley & Sons, 2005.
- [16] Nguyen, Cam. *Analysis methods for RF, microwave, and millimeter-wave planar transmission line structures*. John Wiley & Sons, 2000.
- [17] Bahar, Amyrul Azuan Mohd, et al. "A review of characterization techniques for material's properties measurement using microwave resonant sensor." *Journal of Telecommunication, Electronic and Computer Engineering (JTEC)* 7.2 (2015): 1-6.
- [18] Govind, G., & Akhtar, M. J. (2019). Metamaterial-inspired microwave microfluidic sensor for glucose monitoring in aqueous solutions. *IEEE Sensors Journal*, 19(24), 11900-11907.

- [19] Gao, Wei, et al. "Flexible electronics toward wearable sensing." *Accounts of chemical research* 52.3 (2019): 523-533.
- [20] Mian, Sajjad Hussain, et al. "A novel textile-embedded wearable microwave sensor for non-invasive sweat glucose monitoring." *IEEE Transactions on Instrumentation and Measurement* (2025).
- [21] Van Caekenberghe, Koen. "Modeling rf mems devices." *IEEE Microwave Magazine* 13.1 (2012): 83-110.
- [22] J. Helszajn, *Ridge Waveguides and Passive Microwave Components*. London, U.K.: IEE Press, 2000.
- [23] Vélez, Paris, et al. "Microwave microfluidic sensor based on a microstrip splitter/combiner configuration and split ring resonators (SRRs) for dielectric characterization of liquids." *IEEE Sensors Journal* 17.20 (2017): 6589-6598.
- [24] Mehrotra, Parikha, Baibhab Chatterjee, and Shreyas Sen. "EM-wave biosensors: A review of RF, microwave, mm-wave and optical sensing." *Sensors* 19.5 (2019): 1013.
- [25] Juan, C. G., Grenier, K., Zarifi, M., Ebrahimi, A., & Martin, F. (2025). Planar microwave sensors: State of the art and applications. *IEEE Access*.

### Abbreviations

Symbol	Definition
$\epsilon_{\text{eff}}$	Effective dielectric constant
$\epsilon_{\text{reff}}$	Effective relative permittivity
<b>fr1</b>	Primary resonant mode
<b>fr2</b>	Secondary resonant mode
<b>Z<sub>0</sub></b>	Characteristic impedance
<b>v</b>	Poisson's ratio
<b>Lstrain</b>	Strain-induced inductance
<b>Cstrain</b>	Strain-induced capacitance
$\Delta\epsilon$	Dielectric perturbation
<b>MUT</b>	Material under test
<b>S<sub>11</sub></b>	Reflection coefficient
<b>S<sub>21</sub></b>	Transmission coefficient
<b>VSWR</b>	Voltage standing wave ratio
<b>g<sub>best</sub></b>	Global best particle position in HGPSO
<b>p<sub>best</sub></b>	Personal best particle position in HGPSO
<b>x<sub>i</sub></b>	Particle position vector
<b>v<sub>i</sub></b>	Particle velocity vector
<b>w(t)</b>	Dynamic inertia weight
<b>F(x<sub>i</sub>)</b>	Objective or fitness function
$\Delta\psi$	Fitness improvement threshold